Structure *14*, 953–966, June 2006 DOI 10.1016/j.str.2006.03.016

Single-Molecule Approaches Reveal the Idiosyncrasies of RNA Polymerases

Review

Jordanka Zlatanova,[1,*] William T. McAllister,[2] Sergei Borukhov,[2] and Sanford H. Leuba[3]
[1] Department of Molecular Biology
University of Wyoming
Laramie, Wyoming 82071
[2] Department of Cell Biology
University of Medicine and Dentistry of New Jersey
Stratford, New Jersey 08084
[3] Department of Cell Biology and Physiology
University of Pittsburgh School of Medicine
Hillman Cancer Center
University of Pittsburgh Cancer Institute
Pittsburgh, Pennsylvania 15213

Recently developed single-molecule techniques have provided new insights into the function of one of the most complex and highly regulated processes in the cell—the transcription of the DNA template into RNA. This review discusses methods and results from this emerging field, and it puts them in perspective of existing biochemical and structural data.

Introduction

Transcription, the synthesis of RNA on a DNA template, is the first step in the flow of genetic information in a cell. Transcription is a cyclic process performed by the highly processive, DNA-dependent enzyme RNA polymerase (RNAP) and involves four distinct steps: (1) promoter binding and "closed complex" formation; (2) "open complex" formation and RNA chain initiation; (3) promoter escape and transcript elongation; and (4) termination (Figure 1A). Regulation of transcription can occur at each of these four steps and involves specific nucleotide sequences in the DNA template and/or the nascent RNA transcript, as well as various sets of proteins that bind to the nucleic acids or to the polymerase itself.

Of all of the steps in the transcription cycle, initiation is probably the most complex, as it involves specific promoter recognition and many intermediate transitions before the polymerase achieves a stable elongation state. Elongation, in contrast, does not appear to require as many intermediate steps, nor does it require the large-scale conformational changes that appear to accompany the transition from initiation to elongation. Termination is also a complicated process, and a number of alternative models have been proposed to account for this process.

While initiation has been relatively well studied, elongation is still enigmatic (Uptain et al., 1997; Erie, 2002; Arndt and Kane, 2003; Shilatifard et al., 2003; Greive and von Hippel, 2005). In general, the current view of elongation involves a monotonic mechanism of transcription in which each successive addition of a nucleotide is accompanied by a translocation by one base pair along the DNA template. This monotonic rate of transcription is interspersed with occasional pausing or permanent stalling. The reasons and mechanisms for these interruptions are the subject of extensive biochemical and single-molecule experiments (Reeder and Hawley, 1996; Landick, 1997, 2004; Komissarova and Kashlev, 1997a, 1997b; Nudler et al., 1997; Nudler, 1999; Armache et al., 2005; and see below).

Recent years have witnessed the resolution of the crystal structures of representative polymerases from different sources: T7 phage (Tahirov et al., 2002; Temiakov et al., 2004; Yin and Steitz, 2002, 2004), the thermophilic bacteria *Thermus aquaticus* and *T. thermophilis* (Zhang et al., 1999; Murakami et al., 2002; Vassylyev et al., 2002), and yeast RNAP II (Cramer et al., 2001; Gnatt et al., 2001) (reviewed by Gnatt, 2002; Borukhov and Nudler, 2003). While the crystal structures of the multisubunit RNAPs bear structural homologies among themselves (Figure 1B), the single-subunit RNAPs are structurally unrelated to the multisubunit enzymes. Nevertheless, the transcription process carried out by both classes of RNAPs entails similar molecular mechanisms. Moreover, the two classes of enzymes apparently undergo comparable conformational transitions between initiation and elongation, and they respond to intrinsic termination signals in a similar manner.

Structural comparisons of ternary complexes of the single-subunit T7 RNAP with DNA and RNA that represent consecutive steps of the individual nucleotide addition cycle have revealed in great detail the mechanism for substrate selection, translocation, and helicase activity (Yin and Steitz, 2002, 2004; Tahirov et al., 2002; Temiakov et al., 2004). It is clear that each cycle of nucleotide addition and translocation is associated with movement of particular elements in the corresponding RNAPs. Similar studies for the multisubunit RNAPs are currently in progress and will allow modeling of these enzymes. However, additional experiments will be needed to clarify the nature of the underlying mechanisms of transcription by each of these enzymes.

As elongation occurs, the DNA/RNA hybrid (and the incoming and exiting duplex DNA) translocates with respect to the catalytic center of the polymerase, which involves both longitudinal and rotational movement (Figure 1C). The forward movement of multisubunit RNAPs is frequently interrupted by pausing or arresting at certain template sites. The two states are discriminated by their ability to resume elongation spontaneously. While paused complexes can do this on their own, arrested complexes need extraneous help from protein factors, such as Gre, Mfd, etc. (Borukhov et al., 2005). Pausing may result from a temporary misalignment of the nascent RNA 3′ terminus within the active site, thereby rendering the elongation complex catalytically inactive. This misalignment may occur by several different mechanisms, including (1) RNAP backtracking, in which the RNAP occasionally slides back along the template, keeping the DNA/RNA hybrid in register but extruding the RNA 3′ end through the so-called secondary channel (nucleotide entrance pore); (2) RNAP hypertranslocation, in which the 3′ end of the RNA is shifted away from the catalytic center by one or two nucleotides

*Correspondence: jordanka@uwyo.edu

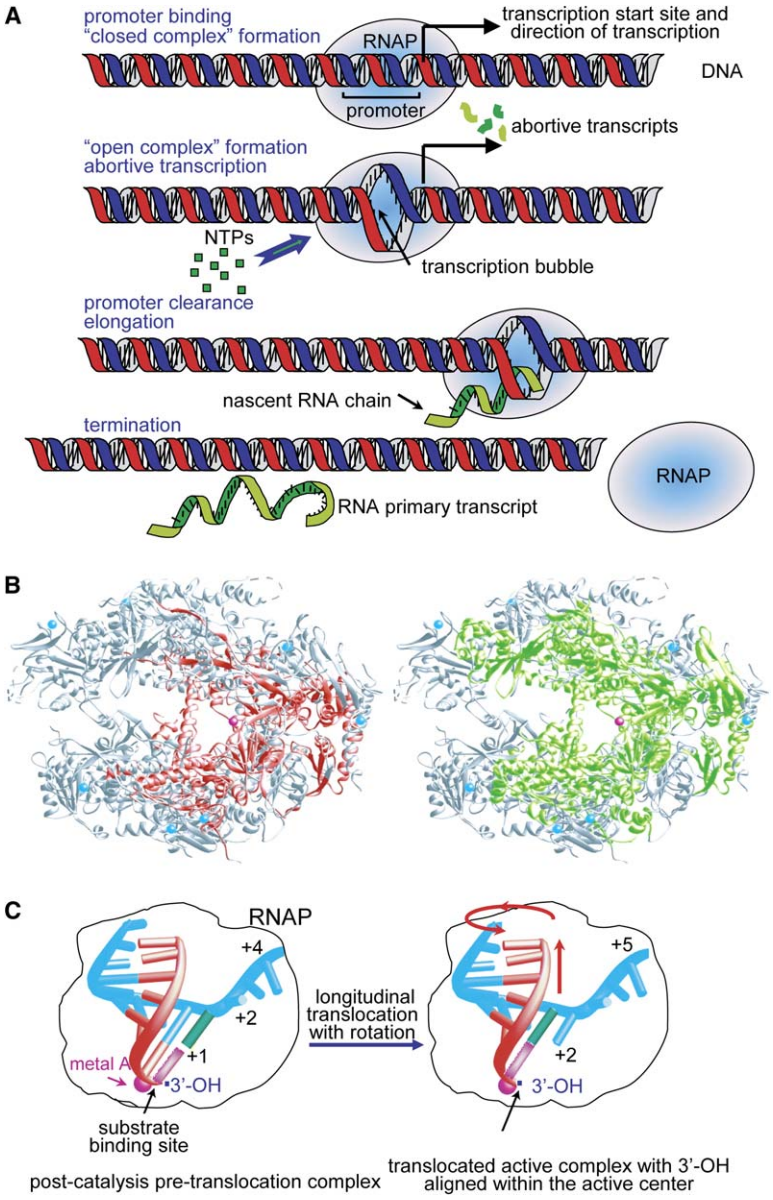

Figure 1. General Overview of Transcription

(A) The phases of transcription. RNAP binds to the promoter region on the DNA to form a "closed complex." RNAP melts the DNA to form the "open complex," in which the DNA strands separate to form a transcription bubble of 13–14 bp. The incoming ribonucleotide triphosphates pair with the exposed DNA bases on the template strand, and the first phosphodiester bonds are formed. At this stage, RNA synthesis is abortive, and the newly formed short transcripts are released from the polymerase. Once the transcript elongates beyond ~15 bases, the polymerase clears the promoter and enters the elongation phase, in which the ternary complex is very stable and the enzyme transcribes long stretches of DNA without dissociating. The characteristic high processivity of RNA polymerase distinguishes it from other DNA-tracking enzymes, such as DNA polymerases and most helicases. Finally, transcription is terminated, resulting in dissociation of the ternary complex.

(B) Comparison between the two largest subunits of a bacterial (*Thermus aquaticus*) (Zhang et al., 1999) and a eukaryotic (*S. cerevisiae*) (Cramer et al., 2001) RNA polymerase (reproduced from Cramer et al. [2001] with permission). The two structures are overlaid; blocks of sequence homology are in red, and regions of structural homology are in green. The structures show considerable conservation around the active center (suggesting a conserved catalytic mechanism), but they differ in the peripheral and surface features, where the polymerases interact with other proteins.

(C) Schematic of the DNA/RNA heteroduplex based on the crystal structure of an elongating RNAP (Gnatt et al., 2001) to illustrate the expected translocation movements of the DNA double helix with respect to the catalytic center of the enzyme (metal A). Left panel, postcatalysis, pretranslocation complex; right panel, translocated active complex. Note that the transition involves two different kinds of motion (red arrows), *longitudinal translocation* along the double helix and *rotation*, so that the 3′-OH group is aligned with the active center and the next nucleotide on the template strand (+2) is oriented properly to determine the chemical nature of the incoming ribonucleotide.

in the upstream direction; or (3) a local distortion or "fraying" of the 3′-terminal nucleotide from the catalytic site without any major lateral movement of the enzyme (see below). To reset the proper alignment and restore forward motion, the polymerase must adjust its position by short-range passive sliding or by cleaving a portion of the nascent RNA (Landick, 1997; Artsimovitch and Landick, 2000). Additionally, at certain template sites, pausing may result from a temporary occlusion of the active site by direct or allosteric effects of mobile structural elements of the RNAP or by extraneous factors (σ70, NusA, Gre, microcin, streptolidigin, etc.) (Ring et al., 1996; Nudler, 1999; Marr and Roberts, 2000; Landick, 2004; Adelman et al., 2004; Mukhopadhyay et al., 2004; Nickels et al., 2005; Bar-Nahum et al., 2005; Tuske et al., 2005; Borukhov et al., 2005). Interestingly, single-molecule studies of T7 RNA polymerase have not revealed such pausing events during elongation, but rather a uniform rate of transcription (Skinner et al., 2004; Thomen et al., 2005; Pomerantz et al., 2005), suggesting that the mode of transcription employed by the multisubunit RNAPs provides a means to regulate these enzymes during elongation.

Extensive biochemical and genetic experiments over the past 20 years have resulted in a large body of information concerning fundamental aspects of transcription. This, coupled with structural information, begins to provide insight into underlying mechanisms of the transcription process and its regulation. However, the available information provides, at best, snap shots along the pathway of the transcription process, and we are still far away from having the seamless cinematographic

picture that would be required to understand the thermodynamics of the nucleotide addition process and the movement of RNAP and the nucleic acid components. These parameters are particularly well suited for investigation by single-molecule methods, which could help address many questions concerning the mechanisms of transcription. For example, what is the force that is generated by RNAP during each cycle of translocation, and what would be the response of the transcription complex to the application of external forces? Would the rate of transcription slow down, or would elongation continue at the same rate until it had reached the limits of thermodynamic opposition (stall force)? What is the rate-limiting step in transcription: is it the catalytic step or the translocation step? What is the basis for the variation in the duration of different pauses on the same DNA sequence—is pausing random, or is it sequence dependent?

The inaccessibility of these questions to current biochemical and structural methods explains the excitement in the field, and why the use of multiple approaches toward understanding the transcription process is so attractive. In this review, we examine the single-molecule approaches that have been used to characterize the transcription process, and we discuss current results and implications.

With the advent of single-molecule techniques and their application to the study of transcription, our understanding of how transcription actually works has deepened considerably. We now envisage RNAP as a powerful molecular motor, capable of exerting both linear and rotary forces on the DNA template to allow threading of the DNA helix through the catalytic center, at the same time rotating the helix by 35° after each catalytic step (Harada et al., 1999; Wang et al., 1998b) (see Figure 1C).

Single-Molecule Techniques Used in Transcription Studies

Development of methods that allow characterization of individual macromolecules is one of the most significant steps in contemporary biology (van Holde, 1999; Science, 1999; Leuba and Zlatanova, 2001). Single-molecule approaches provide direct real-time measurements of high spatial and temporal resolution (nanometer distances, millisecond timescale, and piconewton forces). Rather than measuring population-average properties of molecules in solution (as in conventional biochemical and biophysical methods), these methods assess the properties of individual members of molecular populations, thus allowing insights into the heterogeneity in the functional dynamics of these molecules that were previously unattainable. Equally important, tracking the behavior of one molecule at a time circumvents the need for process synchronization. The significance of this feature of single-molecule methodology cannot be overstated, especially when multistep stochastic processes, such as transcription, are being investigated.

We will briefly describe the principle of action of several single-molecule approaches commonly used to study transcription. In general, there are two categories of methods: those used for observation (atomic force microscope [AFM], tethered particle motion [TPM], and single-molecule fluorescence) versus those that allow mechanical manipulation of the individual molecules in the sample (AFM, optical tweezers [OT], and magnetic tweezers [MT]).

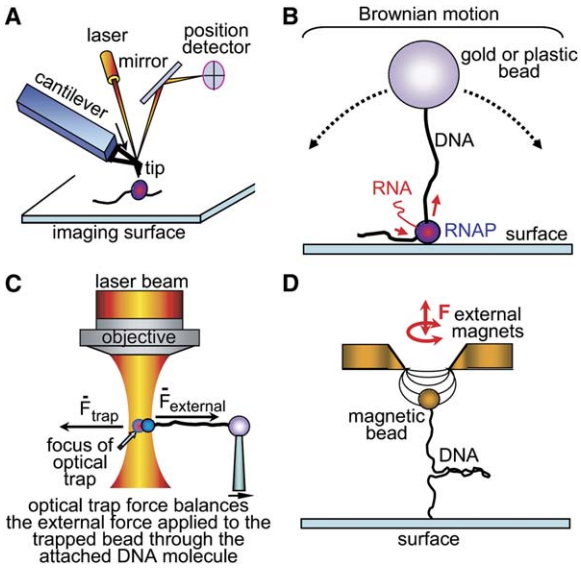

Figure 2. Schematic of the Single-Molecule Approaches Used to Study Transcription

(A) Atomic force microscope (AFM).
(B) Tethered particle motion (TPM) method.
(C) Optical tweezers (OT).
(D) Magnetic tweezers (MT). For further details, see text. Adapted from Zlatanova and Leuba (2003).

In the AFM (Figure 2A), a sharp tip mounted on a flexible cantilever is allowed to scan a sample deposited on an atomically flat surface. Atoms at the tip of the apex experience attractive or repulsive interactions with atoms on the sample, resulting in deflections of the cantilever on which the tip is mounted; these deflections are registered by deflection of a laser beam to create a topographic image. The AFM can also be used to mechanically manipulate biopolymers, or to measure interaction forces between molecular partners (reviewed by Zlatanova et al., 2001).

The TPM method (Figure 2B) is based on the dependence of the extent of Brownian motion of a bead (readily measured by light microscopy) on the length of the DNA template tethering it to the surface. In transcription experiments, the polymerase is immobilized on a glass surface, and a bead is attached to either the upstream or the downstream end of the DNA template; elongation will result in lengthening or shortening of the tether (and a change in the Brownian motion of the bead), depending on the particular geometry used.

In OT, a macromolecule is attached to a plastic bead. The interaction of the bead with a laser beam focused through an objective creates a potential energy well (optical trap) in which the bead is suspended indefinitely; any forced movement of the bead out of this well is counteracted by the optical trap force. Figure 2C depicts how optical trapping can be used to apply (and measure) forces to a macromolecule. To accomplish this, one end of the molecule is attached to the optically trapped bead, while the other end is immobilized to a movable platform (another bead, microscope slide, etc.). As mechanical force is applied to the molecule through

movement of the platform, the force is measured by following the deflection of the laser beam caused by the movement of the trapped bead from its equilibrium position (Ashkin, 1997; Neuman and Block, 2004).

The principle of action of magnetic tweezers (MT) is similar to OT: both kinds of instruments belong to the so-called external field manipulators, in which the molecule is acted upon from a distance, by applying photon (OT) or magnetic (MT) fields to handles attached to the molecules (Bustamante et al., 2000; Zlatanova and Leuba, 2003). In MT (Figure 2D), the DNA is tethered between a surface and a superparamagnetic bead, and the force is applied via external magnets; this set-up also allows for easy introduction of controlled torsion in the molecule by simply rotating the external magnetic field, and thus the bead.

Visualizing Transcription Initiation

Initiation is a complex, multistep process involving: searching for and binding to the specific promoter sequence, melting of the DNA double helix around the site of initiation, formation of the first phosphodiester bond de novo (in the absence of a presynthesized primer, as is the case for DNA polymerases), gradual elongation of the nascent transcript, release of unstable (abortive) initiation products, and, finally, release of promoter contacts and transition to a stable elongation complex. Each of these steps is likely to be accompanied by significant conformational changes in the protein and by changes in the organization of the nucleic acid components of the complex. While many of these steps have been studied by biochemical and physical methods, such as nucleic acid/RNAP photocrosslinking, FRET analysis, electron microscopy, and X-ray crystallography, a complete picture will require the application of single-molecule methods. These would allow insights into such questions as: what is the mechanism by which the polymerase scans the DNA for the promoter sequence; what are the forces that are involved in separating the DNA strands; does the polymerase bend the DNA around the start site; how and when does promoter escape occur; is σ release obligatory for this transition in bacterial transcription complexes? Below, we will discuss single-molecule experiments aimed at studying these processes.

Initiation of transcription has been directly visualized by conventional and cryo-electron microscopy (EM) (Figure 3A) (ten Heggeler-Bordier et al., 1992). Both approaches revealed that promoter binding on supercoiled plasmids resulted in bending of the DNA and the formation of apical loops around the promoter sequence. The observation that the relative orientation of the polymerase and the apical loop (which moves along the DNA template) remained the same during subsequent elongation was interpreted as showing rotation of the DNA around its axis.

Later studies have utilized AFM imaging in buffer to study the mechanism by which the RNAP searches for its promoter (Guthold et al., 1999). (In a broader sense, this problem is encountered by any sequence-specific binding protein looking for its binding sites amid a huge excess of nonspecific DNA). These studies indicate that the promoter search involves a one-dimensional diffusion mechanism, in accordance with earlier studies employing fluorescence microscopy. Kabata et al. (1993) observed a sliding motion of individual fluorescently labeled RNAP molecules on combed arrays of linear λ-DNA molecules. In a more sophisticated approach, Harada et al. (1999) observed RNAP binding to DNA by combining OT to suspend a single λ-DNA molecule above the surface and total internal reflection to excite fluorescently labeled RNAPs. These authors reported dissociation rate constants that differed on promoter regions versus regions of nonspecific DNA; for the nonspecific regions, the association and dissociation constants depended on the AT content of the region. The authors also observed that the direction of movement along the DNA was random at nonspecific binding sites, indicating thermally driven diffusion, and arguing for a one-dimensional sliding search mechanism.

A recent report used OT to study the mechanism of this one-dimensional search (Sakata-Sogawa and Shimamoto, 2004). In this set-up, DNA molecules were attached to optically trapped beads and dragged over a surface coated with immobilized *E. coli* RNAP molecules. Under certain conditions, the enzyme slid along the DNA; this sliding occurred as a result of tracking a DNA groove as evidenced by the generation of torque (resulting in rotation of the bead). Taken in their entirety, these data indicate that the mechanism of promoter search involves thermally driven sliding of the enzyme along the DNA, tracking a DNA groove.

A number of biochemical methods, neutron scattering, and conventional EM have indicated that the promoter region becomes bent upon bacterial RNAP binding (for references, see Rippe et al., 1997; Schulz et al., 1998; Rivetti et al., 1999; Coulombe and Burton, 1999). AFM imaging of nonspecifically bound RNAP holoenzymes, and of closed and open promoter complexes, has provided a measure of DNA contour length reduction (compared with the respective naked DNA molecule containing the promoter) and of bend angles (Rivetti et al., 1999). Although the actual numbers differ, depending on the imaging conditions, and possibly on the type of σ subunit (σ^{70} versus σ^{54}), it seems that the degree of bending changes upon the transition from nonspecific to specific binding, and from closed to open complexes. These data, taken together with the DNA contour length reduction, have been interpreted in support of the notion that promoter DNA wraps almost a full turn ($\sim$300°) around the polymerase (Rivetti et al., 1999). In a continuation of these studies, Rivetti et al. (2003) investigated the degree of DNA wrapping in elongation complexes that were stalled at different positions of the template. The DNA deformation was compatible with $\sim$180° wrapping, i.e., less than that observed in open promoter complexes.

Recent studies by Kapanidis et al. (2005) addressed a controversial question of how and when σ is released during the transcription cycle (Mooney et al., 2005). The authors applied a single-molecule assay by using leading-edge/trailing-edge FRET with alternating-laser excitation to determine the position of RNAP on DNA and, at the same time, detect the presence of σ^{70} in the initiation, early elongation, and mature elongation complexes. The results indicate that a substantial fraction (50%–90%) of elongation complexes retain σ^{70}, arguing, therefore, against obligate σ release and supporting a hypothesis that stable σ-RNAP complexes may persist throughout the transcription cycle.

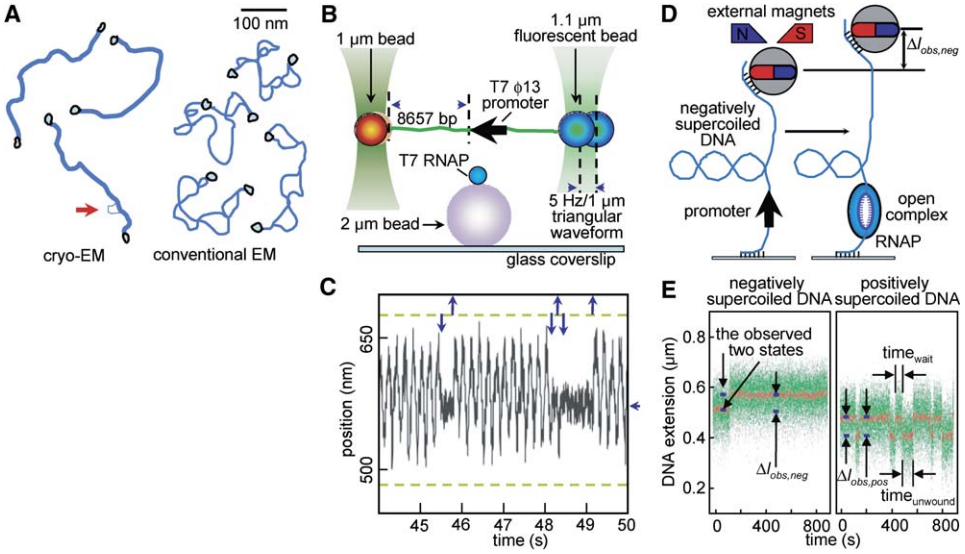

Figure 3. Visualizing Promoter Binding and/or Melting by Individual Polymerase Molecules

(A) Illustrations of micrographs of supercoiled pUC DNA with *E. coli* RNA polymerases bound to the two active promoters: the interaction causes the formation of an apical loop around the promoter. The enzyme molecules are visible as dense blobs, generally located at an apex of the supercoiled DNA. Left-hand side: illustration of micrograph obtained by cryo-electron microscopy of DNA molecules suspended in vitrified solution; the molecules are tightly supercoiled, so that the two DNA helices are not resolvable. The asymmetry of the promoter locations is seen as a short loop (arrow) in the otherwise interwound molecule. Right-hand side: illustration of electron micrographs of DNA molecules adsorbed to a positively charged carbon film, dried, and rotary shadowed; note that the molecules appear more loosely supercoiled due to surface adsorption effects. Adapted from work by ten Heggeler-Bordier et al. (1992).

(B) Experimental set-up of the OT system of Skinner et al. (2004). A single DNA molecule is tethered between two beads held by independently controlled optical traps. The fluorescently labeled bead (right) allows the upstream end of the DNA molecule to be identified prior to transcription initiation by viewing in epifluorescence mode. The partially extended DNA template that contains a T7 promoter is maneuvered so that the central region is touching the RNAP-coated, surface-immobilized bead. A triangular waveform is then applied to the upstream bead, causing it to oscillate, while the position of the (left) downstream bead is monitored with a four-quadrant photodiode to detect DNA binding. Interaction events are detected as a "decoupling" of the motion of the downstream bead from the driven upstream bead. Adapted from work by Skinner et al. (2004).

(C) Broken lines indicate the range of displacement of the downstream bead during coupled bead motion (trap center at position = 675 nm), i.e., when the DNA is not bound by the polymerase. When the DNA binds to the enzyme, the oscillations of the downstream bead cease as it becomes upcoupled from the oscillations applied to the upstream bead. Rapid dissociation and reassociation events are often observed (see downward and upward arrows) (reproduced with permission from Skinner et al. [2004]). This figure is a bitmap scan of original data traces; however, slight changes were made to the fonts and graph markings.

(D) Experimental set-up of the MT system of Revyakin et al. (2004). A double-stranded DNA molecule containing a single promoter is topologically constrained between a paramagnetic bead at one end and a glass surface at the other end. A stretching force is applied to the DNA tether via a pair of external magnets. The DNA end-to-end extension (*l*) is monitored in real time by videomicroscopy as the distance between the bead and the surface. Controlled rotation of the magnets rotates the bead, thus introducing supercoiling into the DNA: the formation of plectonemes leads to changes in *l*. In a torsionally constrained DNA molecule with constant linking number (*Lk*), a change in twist (*Tw*; number of times the two DNA strands cross each other in the double-helical structure) must be compensated by an equal, but opposite, change in writhe (*Wr*; number of supercoils). With negatively supercoiled DNA, unwinding of ~1 turn of promoter DNA by RNAP (promoter opening) must result in a compensatory loss of ~1 negative supercoil and, correspondingly, an increase in *l* ($\Delta l_{obs,neg}$). With positively supercoiled DNA, promoter opening will result in a compensatory gain of one positive supercoil, i.e., a decrease in *l* will be observed (not shown). Adapted from work by Revyakin et al. (2004).

(E) DNA extension versus time plots indicating promoter opening by RNAP. Left-hand side: promoter opening on negatively supercoiled DNA is stable and effectively irreversible. Right-hand side: unstable, reversible promoter opening on positively supercoiled DNA. Green points, raw data obtained at a video rate of 30 frames/s; red points, averaged data (1 s window); T_{wait}, time interval between a rewinding event and the next unwinding event; $T_{unwound}$, time interval between an unwinding event and the next rewinding event (reproduced with permission from Revyakin et al. [2004]). This figure is a bitmap scan of original data traces; however, slight changes were made to the fonts and graph markings.

Dynamic Measurements of Promoter Binding and Opening

Two recent papers used dynamic methods to analyze promoter binding. Skinner et al. (2004) used a sophisticated three-bead experimental set-up (Figures 3B and 3C; Table 1) to study the kinetics of promoter binding, initiation, and elongation involving the same individual T7 RNAP molecule. The transition from initiation to processive elongation manifested itself as a lag phase, much longer than the mean lifetime of the RNAP-promoter complex, identifying the isomerization of the stationary initiation complex to an elongating one as a rate-limiting step.

Another approach to observing promoter melting and clearance by RNAP made use of the topological properties of a DNA molecule constrained between a surface and a magnetic bead in a MT set-up (Revyakin et al., 2004) (Figures 3D and 3E). Conservation of the linking number in a torsionally constrained DNA molecule requires that a change in twist in the double helix be compensated by an equal change of opposite sign in writhe (supercoiling). If the polymerase binds to a negatively supercoiled DNA molecule (the supercoiling being preintroduced by controlled rotation of the external magnetic field) and unwinds ~1 turn of promoter DNA, the compensatory introduction of one positive supercoil

Table 1. Major Reported Single-Molecule Transcription Elongation Experiments

Experimental System and Approach	Main Observations	Conclusions/Interpretations	Reference
Gold particles (40 nm) attached to upstream end of DNA templates transcribed by immobilized *E. coli* RNAP, following release from stall; analysis of the Brownian motion of the particles by the light microscopy (TPM) method	The extent of Brownian motion increases with time after the addition of NTPs; the frequent detachment of particles from the surface is interpreted as termination; measured elongation rates are consistent with solution values	The intrinsic elongation rate of individual molecules does not vary substantially with time; no substantial random pausing	Schafer et al., 1991
Technical improvements of the TPM method of Schafer et al. (1991): 0.23 μm polystyrene beads, improved sample preparation, faster data collection (Figure 2B)	Empirical validation of the TPM method for tether lengths of 308–1915 bp; determination of the accuracy and precision of the method; elongation rate measurements (Figure 4B)	Linear dependence between Brownian motion and tether length; broad distribution of elongation rates among individual RNAP molecules	Yin et al., 1994
Stalled *E. coli* RNAP immobilized on coverslip; downstream DNA end attached to optically trapped 0.5 μm bead; the force applied to trapped bead opposes elongation	During elongation, the bead is pulled away from the trap center due to shortening of the downstream DNA; at saturating NTP (1 mM) concentrations, the enzyme stalls reversibly at ~14 pN[a]	The stall forces for RNAP are much larger than those measured for kinesin and myosin; the ability of RNAP to exert forces and its energy conversion efficiency place the enzyme in the category of mechanoenzymes (molecular motors)	Yin et al., 1995
Experimental geometry as in Yin et al. (1995); the first use of a feedback-controlled optical trap for dynamic F-V measurements (Figure 5A)	Single-molecule records display periods of steady elongation (at constant rate) interrupted by pauses at both low and high loads (Figure 5B); F-V curves are convex, i.e., velocity is independent of load to a force approaching stall; stall forces are broadly distributed	Mechanical stall is interpreted as an elongation-incompetent (backtracked) state branching off the elongation pathway (see Figure 6)	Wang et al., 1998b
Prestalled *E. coli* RNAP complexes imaged in the absence and presence of NTP; AFM time-lapse sequences (Figure 4A)	RNAP remains stably bound to the mica surface, while DNA is transported through it; a comparison with solution experiments shows a somewhat lower activity of the immobilized enzymes; the pattern of pauses and termination are also affected by the surface	Transcription can be directly visualized by AFM; estimate of frictional drag force experienced by RNAP	Kasas et al., 1997; Guthold et al., 1999
Prestalled *E. coli* RNAP complexes attached to a bead held by a pipette with the downstream end of DNA attached to another bead; forces opposing transcription are applied to downstream bead by flow (Figure 4C)	Contour-length versus time curves show variable elongation rates along the DNA template, interspersed with pauses (Figure 4D); peak rates for individual RNAPs differ significantly; no effect of force on these rates up to stall forces	Elongating RNAPs switch between more competent or less competent transcription states; conversion between these two states is slow; reversible pausing[b] is a kinetic intermediate between elongation and an arrested state (irreversible stops)	Davenport et al., 2000
Real-time optical microscopy observation of rotation of a magnetic bead attached to downstream DNA; *E. coli* RNAP immobilized to the surface (Figures 4E and 4F); elongation rate determined in solution or by following changes in tether length (Brownian motion)	Large variation in rotation rates among individual RNAPs (including pausing)	The relationship between elongation rate and rotation rate is interpreted in terms of high-fidelity tracking of the right-handed DNA helix; calculations estimate torque > 5 pN·nm[c]	Harada et al., 2001
Prestalled *E. coli* RNAP complexes attached to a bead held by a pipette, with either the downstream or the upstream end of DNA attached to another bead; opposing or assisting forces applied to this second bead by flow	The overall elongation rate (including pauses) is strongly force and NTP dependent; however, there is no force dependence for pause-free elongation rates; assisting force reduces the efficiency of both pausing[b] and arrest	Force (either opposing or assisting) does not affect translocation along the main elongation pathway; arrested molecules cannot be rescued by force, suggesting that, in addition to backtracking, there is a force-independent conformation change of the enzyme or the complex during arrest	Forde et al., 2002
Hemagglutinin-tagged stalled *E. coli* RNAP attached to a coverslip via anti-HA antibody; the downstream end of DNA is attached to a trapped bead; optical trapping experiments at a constant force of 4 pN	During periods of uninterrupted movements (no pausing), the traces of individual molecules have similar slopes; a mutant enzyme pauses more frequently and elongates more slowly	Individual RNAPs exhibit similar elongation rates; differences in overall rates are attributed to statistical variation in the frequency and duration of pauses	Adelman et al., 2002

Table 1. *Continued*

Experimental System and Approach	Main Observations	Conclusions/Interpretations	Reference
T7 RNAP transcribes DNA combed by low capillary forces (DNA extension close to its contour length); elongation is visualized by fluorescently labeling nascent RNA	No transcription can occur on overstretched DNA or on nonspecific DNA that does not contain T7 promoters		Gueroui et al., 2002
E. coli RNAP or yeast pol III complexes stalled in solution at different positions of the template are imaged with the AFM.	Analysis of stalled elongation complexes shows "DNA compaction" of ~22 nm for *E. coli* RNAP and ~30 nm for pol III; wide DNA bend angle distributions with averages of 50°–65°; when RNAP is stalled far from the promoter, the nascent RNA chain is also visible, exiting inside the large angle between upstream and downstream DNA	DNA compaction and DNA bend angles compatible with ~180° DNA wrapping around the enzyme; this is less than the 300° wrapping in the open promoter complex; implications for transcribing through a nucleosome	Rivetti et al., 2003
Biotinylated derivative of *E. coli* RNAP attached to optically trapped 500 nm beads; either the upstream or downstream end of DNA of the stalled complex is attached to surface (Figure 5C); high spatial (~1 bp) and temporal resolution; pauses as short as ~1 s can be discerned	Elongation rate varies among molecules; individual RNAPs do not switch between slow and fast states; the majority of pauses are short and randomly distributed along the template (ubiquitous) (Figure 5D)	Since neither the probability nor the duration of the ubiquitous pauses is force dependent, they are proposed to be caused by structural rearrangement in the enzyme, rather than by backtracking (Figure 6)	Neuman et al., 2003
Biotinylated derivative of *E. coli* RNAP attached to the smaller of two beads; either the upstream or downstream end of DNA is attached to the other bead; the beads are independently optically trapped; tension applied through the larger bead[d] (Figure 5E)	5% of pauses are longer than 20 s; backtracking occurs upon entry into long (but not short, see above) pauses; three phases of motion within long pauses are discernable: (i) backtracking, (ii) pausing per se, and (iii) slow recovery (Figure 5F)	The duration and frequency of the backtracking pauses are strongly dependent on the application of either opposing or assisting force (in contrast to the short pauses case); the backtracking nature was confirmed by the effects of ITP incorporation and the presence of GreA and/or GreB	Shaevitz et al., 2003
Three-bead geometry (Figure 3B): DNA tethered between two optically trapped beads is held near a third bead coated with T7 RNAP (this bead is immobilized on a surface); triangular oscillation is applied to the upstream bead, and the position of the downstream bead is monitored	The oscillation of the downstream bead ceases when interaction with RNAP occurs (Figure 3C); a population of long-lived DNA bound complexes is engaged in elongation (seen as displacement of the downstream bead from the trap due to the shortening of the DNA tether)[e]	Mean transcription rates for the six elongation events observed are very similar; no evidence of reversible pausing is seen	Skinner et al., 2004
T7 RNAP transcribing against an opposing force in an OT set-up	Force acts as a competitive inhibitor of NTP binding	Data argue against the power stroke model for translocation	Thomen et al., 2005
Confocal microscopy with two-color alternating laser excitation to simultaneously monitor spFRET and fluorophore stoichiometry in transcription complexes; labeling on (i) the leading edge of *E. coli* RNAP and the downstream end of the DNA template, or (ii) the trailing edge of RNAP and the upstream DNA end	A large fraction of both early and mature elongation complexes retains σ70; the half-life of σ70 retention is long, suggesting that some complexes may retain the subunit throughout elongation	σ70 release is not an obligatory step in promoter escape, but is rather a stochastic event that occurs throughout elongation; both mechanistic and functional implications are discussed	Kapanidis et al., 2005
An ultrastable OT system is constructed by using the dumbbell geometry of Shaevitz et al. (2003), enclosure of optical elements in a helium box, and an all-optical arrangement for constant force feedback control	Distance versus time records of single molecules of *E. coli* RNAP show discrete steps of ~3.7 ± 0.6 Å, corresponding to the mean rise per base pair in B-DNA	RNAP advances along template DNA in single base pair steps; global fits of F-V data at varying concentration of NTPs are consistent with Brownian ratchet mechanisms of translocation and argue against power stroke mechanisms	Abbondanzieri et al., 2005

[a] Movement sometimes slowed gradually during approach to F_{stall}, in other cases, the stop was abrupt.
[b] Analysis restricted to relatively rare lengthy pauses (see Neuman et al., 2003).
[c] Apparent saturation of rotation rate at 0.2 rps explained by RNAP reaching its maximal torque at this rotation rate.
[d] None of the components of the assay were attached to the coverglass surface, isolating the system from drift (leading to near-base-pair resolution).
[e] The only work that directly observed promoter binding, initiation, and elongation by a single RNAP molecule.

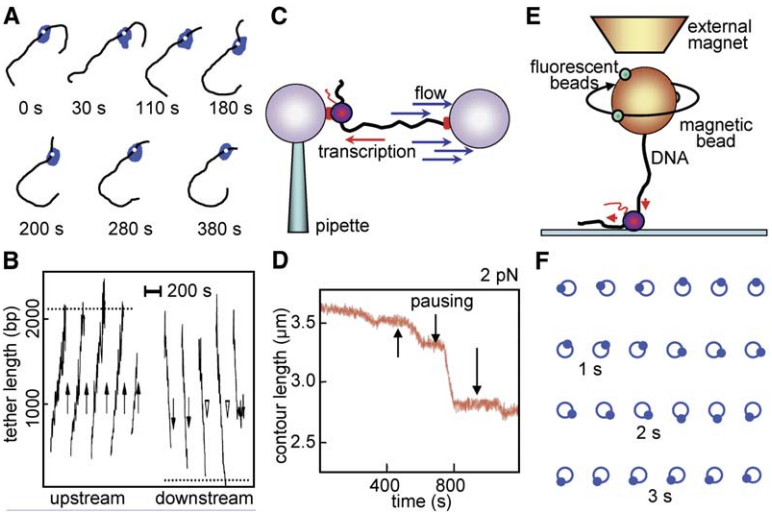

Figure 4. Following Transcription Elongation on Single DNA Molecules in Real Time

(A) Schematic drawing of AFM images of *E. coli* RNA polymerase transcribing naked DNA (data adapted from work by Guthold et al. [1999]). From left to right: a stalled RNAP complex, before injection of NTPs into the liquid cell, and consecutive images of transcription elongation complexes (after NTP injection), with the RNAP bound to the surface and the DNA threaded though the active center of the enzyme. The stalling site is asymmetrically located on the DNA template, making it possible to identify the direction of transcription.

(B) Transcription elongation as measured by the TPM method. Example tether-length/time courses with the bead at the upstream (left traces) or downstream (right traces) end of the template (reproduced with permission from Yin et al. [1994]). This figure is a bitmap scan of original data traces; however, slight changes were made to the fonts and graph markings. Dashed lines indicate expected final tether lengths. Arrows and open triangles point to the time when the bead was released from or became stuck to the glass slide surface, respectively.

(C) Schematic of the videomicroscopy flow experiments as used by Bustamante and colleagues (Davenport et al., 2000). A stalled *E. coli* RNAP carrying its template and the nascent RNA chain is attached to a 2.2 μm bead held in a pipette. The downstream end of the template DNA is attached to another bead, to which hydrodynamic drag force can be applied via a computer-controlled flow. Transcription is reinitiated by the addition of NTPs and observed as shortening of the DNA tether between the beads. Adapted from work by Davenport et al. (2000).

(D) Raw data from a transcription experiment. The arrows denote temporal pauses in elongation (reproduced with permission from Davenport et al. [2000]). This figure is a bitmap scan of the original data traces (insert removed); however, slight changes were made to the fonts and graph markings. 2 pN indicates the force at which the example data trace was collected.

(E) Schematic of the MT experiment performed to follow the relative rotation of the DNA with respect to the polymerase (Harada et al., 2001). A stalled *E. coli* polymerase is immobilized onto a glass surface, and a small magnetic bead is attached to the downstream end of the template in a way that allows torque transmission to the bead. To visualize rotation by videomicroscopy, the magnetic bead is decorated with smaller fluorescent beads. Adapted from work by Harada et al. (2001).

(F) Schematic illustrations of snapshots of rotating beads reflecting the rotation of the DNA double helix within the elongating polymerase molecule. Adapted from work by Harada et al. (2001).

will manifest itself as a loss of one of the preexisting negative supercoils; thus, the length of the tether will increase by a readily recordable amount. This approach, also applicable to an initially positively supercoiled DNA tether, converts an effectively undetectable change in local DNA geometry to an observable change in bead position, thus amplifying the signal enormously. As Figure 3E indicates, promoter melting on negatively supercoiled DNA is stable, and practically irreversible, whereas melting on positively supercoiled DNA is very unstable and reversible, as expected from thermodynamic considerations.

Transcription Elongation as Studied by Single-Molecule Approaches

Most of the published single-molecule work deals with the elongation process. This is largely because complexes that are suitable for such studies may readily be formed by initiating on templates that allow the polymerase to proceed a defined distance downstream from the promoter in the presence of a limiting mixture of substrate nucleotides (the polymerase stalls at the first position of the template where the corresponding nucleotide is missing). Such halted elongation complexes are highly stable and may resume transcription upon addition of the missing nucleotide(s) directly in the liquid cells of the instruments.

A detailed description of the major single-molecule elongation experiments is provided in Table 1. Here, we summarize the main approaches and focus on a number of questions for which single-molecule techniques are likely to prove particularly valuable. Of particular interest is the question of whether all RNAPs in a population move at the same rate, or whether individual molecules may move with variable rates.

Elongation has been studied by a variety of single-molecule approaches: AFM, TPM method, flow- or fluorescence-videomicroscopy, MT (Figure 4), and OT (Figure 5). The TPM method (Figure 2B) provided the first real-time observation of transcription elongation (Figure 4B) (Schafer et al., 1991; Yin et al., 1994) and suggested that the kinetic properties of individual RNAP molecules in a putatively homogeneous population varied to a larger degree than expected on the basis of the experimental uncertainty of the rate measurements. Recent modifications to the TPM method to avoid the use of immobilized enzymes (and thus a potential artifactual source of enzyme heterogeneity) (Tolic-Nørrelykke et al., 2004) strengthened the conclusion that an RNAP population contains multiple kinetically (and possibly structurally) distinct individual molecular species (see discussion below).

Videomicroscopy flow experiments from Bustamante's laboratory (Davenport et al., 2000; Forde et al., 2002) (Table 1) were aimed at studying pausing and arrest during elongation by *E. coli* RNAP and the effect of applied assisting or opposing force on translocation rates. The experimental approach is illustrated in Figure 4C, and an example elongation curve (change of tether length as a function of time) is presented in Figure 4D. Whereas the reported effect of force on translocation rate confirmed previous OT results (Yin et al.,

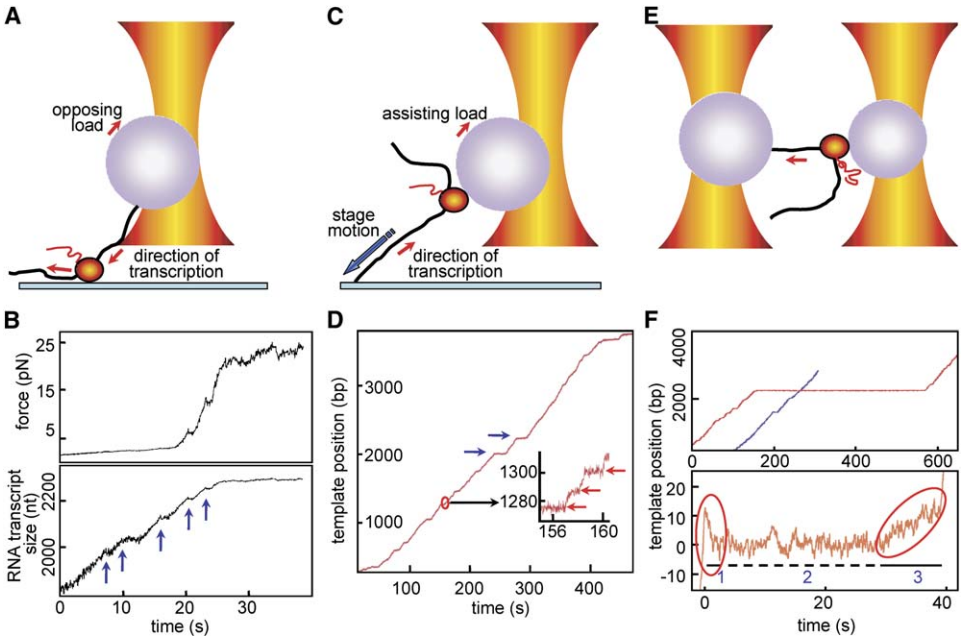

Figure 5. Transcription Elongation and Pausing Studied by OT

(A) Cartoon of the set-up of Wang et al. (1998b) (adapted). A stalled ternary complex of *E. coli* RNAP, the DNA template, and a nascent RNA chain is fixed to a glass surface inside a flow cell. The polystyrene bead, attached to the downstream end of the DNA, is held by the optical trap. As transcription proceeds, DNA is threaded through the active center of the enzyme. In this configuration, the trap applies an opposing load.

(B) Force and corresponding transcript length as a function of time at high load (reproduced with permission from Wang et al. [1998b]). Data recorded in a feedback-controlled instrument, in which the bead position is actively maintained by changing the trap stiffness (i.e., the force applied to the bead) as transcription occurs. Force increased until the complex stalled at ~23 pN. The arrows in the transcript size trace indicate transcriptional pauses. This figure is a bitmap scan of original data traces; however, slight changes were made to the fonts and graph markings. Only the original traces with pauses are shown.

(C) Concept of the experiments of Neuman et al. (2003) (adapted). The transcribing polymerase is attached to a polystyrene bead, and the upstream end of DNA to the surface of a flow cell. The bead is held in the optical trap at a predetermined position from the trap center, thus, the bead experiences a restoring force toward the trap. The movement of the enzyme along the immobilized template causes bead displacement that is compensated for by both horizontal and vertical movement of the stage. In this configuration, the trap applies an assisting load. Attaching the downstream end of the DNA to the surface applies hindering force.

(D) A template position versus time trace for a single polymerase transcribing a 3.5 kbp template under a 18 pN hindering force (reproduced with permission from Neuman et al. [2003]). The blue arrows indicate seconds-long pauses; the red arrows in the blow-up show shorter (~1 s) pauses. This figure is a bitmap scan of original data traces (upper insert removed); however, slight changes were made to the fonts and graph markings.

(E) Concept of the experiments of Shaevitz et al. (2003) (adapted). Two beads are held in separate optical traps, with the right trap being ten times weaker. In the geometry depicted, the smaller (right) bead is attached to a single RNAP, and the larger (left) bead is attached to the downstream end of the DNA; this set-up applies an opposing force. Transcript elongation pulls the beads together, with almost all motion appearing as displacement of the weakly trapped right bead.

(F) Upper panel: records of two individual RNAP molecules (red and blue) transcribing the same template (reproduced with permission from Shaevitz et al. [2003]). A very long pause is seen in the red trace. Lower panel: backtracking, occurring only upon entry into the long pauses. Phase 1, solid line, backtracking; phase 2, dotted line, pause; phase 3, solid line, recovery. This figure is a bitmap scan of original data traces; however, slight changes were made to the fonts and graph markings. Phases 1 and 3 are highlighted by red ovals.

1995; Wang et al., 1998b), measurements of elongation rates suggested that individual polymerase molecules might change their intrinsic elongation rates along the template, a concept that generated considerable controversy. The TPM studies mentioned above (Schafer et al., 1991; Yin et al., 1994; Tolic-Nørrelykke et al., 2004) and some more recent studies (Neuman et al., 2003; Shaevitz et al., 2003) show that individual molecules exhibit a broad range of intrinsic elongation rates that remain constant for each enzyme during elongation. (For reviews on the biochemical data on this issue, the reader is referred to works by von Hippel and Pasman [2002] and Greive and von Hippel [2005]).

A recent paper by Block and collaborators (Abbondanzieri et al., 2005) has reported on the development of an ultrastable OT system that allows unprecedented ångström-level resolution. Elongation records taken at this resolution resolve discrete steps of ~3.4 Å, providing the first experimental measurement of the translocation step size of RNAP: the addition of each nucleotide to the nascent RNA is accompanied by a forward movement of the RNAP along the DNA by a single base pair.

An overview of the published single-molecule data leads to the following two conclusions: (1) there is a broad, unimodal distribution of elongation rates among individual members of an RNAP population; and (2) individual polymerases are likely to transcribe at a constant velocity throughout elongation (not taking into accounts pauses and arrests, see below).

In addition to issues concerning the linear movement of the RNAP along the DNA template, there are questions regarding the rotational movement of the RNAP with respect to the helical axis of the DNA. There exist possible scenarios of movement of the enzyme during

elongation that do not imply precise helical tracking (discussed by Harada et al., 2001). Real-time fluorescence microscopy in an MT apparatus was employed to visualize the rotation of the DNA template by *E. coli* RNAP (Harada et al., 2001) (Figures 4E and 4F; for concept of DNA rotation by the polymerase, see Figure 1C; Table 1). The authors compared *rotation rates* (revolutions of the magnetic bead per second) averaged over a population of individual molecules at a certain NTP concentration with averaged *elongation rates* recorded at the same NTP concentrations (the elongation rates were measured either in bulk solution or by following the Brownian motion of a nonmagnetic bead under the conditions used for the rotation experiments). If the enzyme faithfully tracks the DNA double helix, the rotation rate should be equal to the elongation rate divided by 10.4 (the number of base pairs per helical turn). Indeed, the calculated value of 8.7 ± 3.7 nucleotides per revolution supports (within experimental error) high-fidelity tracking, with the RNAP exerting a torque of >5 pN·nm.

Force Dependence of Transcription Elongation

Many of the original OT experiments were set up to determine the dependence of elongation (i.e., *translocation*, since what are measured are changes in tether length, not actual catalysis) on applied force. The application of force to the template is expected to specifically affect the rates and equilibrium constants of conformational transitions—such as backtracking—responsible for RNAP movement relative to its template, and may thus lead to a better molecular definition of the separate steps in the process.

The mechanism by which RNAP translocates during elongation, and how the necessary force is generated, is the subject of current controversy. In general, two types of models have been proposed to account for translocation. The first (power stroke) mechanism suggests that a conformational change in the enzyme coupled to pyrophosphate release at the end of each nucleotide addition cycle drives translocation (Yin and Steitz, 2004). The second (Brownian ratchet) mechanism proposes that the elongation complex may exist in equilibrium between pre- and posttranslocated states, and that it oscillates back and forth (over a distance of a few base pairs) along the template by a thermally driven sliding mechanism. Binding of the incoming NTP serves as a stationary pawl that prevents reverse sliding of RNAP relative to the nucleic acid scaffold, thus preferentially stabilizing the posttranslocated state (Guajardo and Sousa, 1997; Holmes and Erie, 2003; Bai et al., 2004; Bar-Nahum et al., 2005). In multisubunit RNAPs, it has been suggested that mobile elements in the RNAP (e.g., the F bridge at the 3′ face of the DNA/RNA hybrid) may act as a second, reciprocating-type pawl through reversible conformational transitions (Gnatt et al., 2001; Bar-Nahum et al., 2005). A number of recent experiments using single-molecule methods to explore the effects of force and nucleotide concentrations on translocation have been performed (e.g., Thomen et al., 2005; Abbondanzieri et al., 2005); these studies favor the Brownian ratchet mechanism and its variants.

Yin et al. (1995) and Wang et al. (1998b) used two different modes of operation of an OT instrument to conduct static measurements of the stall force (operationally defined as the opposing force that leads to cessation of translocation) or dynamic measurements of the dependence of elongation velocity on force (Figures 5A and 5B; Table 1). In addition to providing the first measures of RNAP strength (stall force between 15 and 30 pN), these studies unraveled the convex character of the force-velocity (F-V) curves and showed that velocity remains nearly independent of load up to a significant force, approaching stall. Mechanical stall was interpreted as an elongation-incompetent state branching off the main reaction pathway, in agreement with models based on biochemical data (the convex shapes of the F-V curves were suggested to arise because the rate-limiting biochemical transition is not load dependent, only the translocation steps are (for theory, see Jülicher and Bruinsma, 1998; Wang et al., 1998a; Bustamante et al., 2004); in such models, the enzymatic turnover remains independent of force until the load-dependent process slows to the point at which its rate becomes comparable to the rates of biochemical reactions. Thus, the convex character of the F-V curves indicates that the translocation step is *not* rate limiting in transcription elongation. It should be noted that other molecular motors, such as kinesin or the phage ϕ29 packaging motor, exhibit different shapes of the F-V curves, suggesting underlying differences in mechanisms (for further detailed discussion, see Bustamante et al., 2004).

RNAP Pausing, Arrest, and Termination

RNAP pausing and arrest have attracted considerable attention because of (1) the importance of these events in regulation of overall elongation, (2) the wealth of available biochemical data, (3) availability of theoretical models treating pausing and arrest as pathways branching off the main elongation pathway, and, last, but not least, because of (4) the relative ease of observing, recording, and analyzing pausing in single-molecule kinetic traces. Table 1 presents the available data, and Figures 5A–5F illustrate the experimental geometries and some raw kinetic data obtained from OT experiments. As can easily be seen, the smooth forward movement of the enzyme is often interrupted by pauses of different durations.

Two recent papers from Block's laboratory report detailed analysis of high-resolution OT data on transcriptional pausing (Neuman et al., 2003; Shaevitz et al., 2003). The experimental geometries used are depicted in Figures 5C and 5E, and respective example curves are shown in Figures 5D and 5F, respectively. The first study (Neuman et al., 2003) focuses on ubiquitous short pauses, whereas the second one (Shaevitz et al., 2003) describes long pauses during which the RNAP backtracks along the template, with extrusion of an already synthesized portion of the RNA transcript from the catalytic center (short and long pauses are operationally defined as those having a duration shorter than 5 s or longer than 20 s, respectively). The combined data from the two studies lead to a thorough description of the nature of these two kinds of pauses, and they support and further elaborate on the biochemical results (Figure 6; Table 2). Several important points on the long-lived pauses warrant further discussion.

Sophisticated averaging procedures allowed probing details of RNAP motion that would have remained

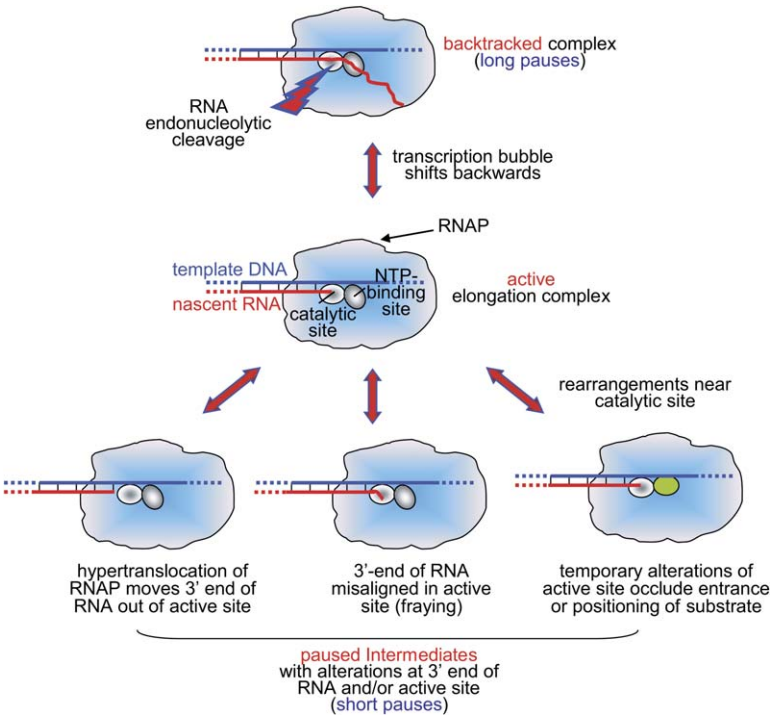

Figure 6. Illustration of the Conformational States of the RNA Polymerase Elongation Complexes

This figure is based on biochemical studies (Erie, 2002) and the single-molecule studies of Neuman et al. (2003) and Shaevitz et al. (2003). In the transcriptionally active complex, the 3′ end of the nascent transcript is properly aligned within the catalytic center of the enzyme, allowing for efficient elongation. Slight conformational rearrangements near the catalytic site cause displacement of the 3′ end from its proper position, slowing down transcription (this state has been termed the "unactivated" state [Erie, 2002]); this is allegedly the state inhabited by the frequently occurring short pauses. If the transcription bubble shifts backward along the DNA/RNA heteroduplex (backtracking), the 3′ end of the transcript finds itself extruded through the secondary channel of the enzyme; this state is inactive because of the long-range misalignment of the RNA end and the catalytic site. Complexes halted at this stage can resume transcription only after the RNA tail is removed by the endonucleolytic action of the polymerase, a reaction stimulated by factors such as GreA and GreB from bacteria and TFIIS from eukaryotic cells. The recovery is slow, with the initial synthesis of the RNA portion that had been chopped off being many-fold slower than the normal continuous elongation process.

Table 2. Characteristic Features of Short and Long Transcriptional Pauses

Feature	Short Pauses	Long Pauses
Frequency of occurrence	~1 per 100 bp	~1 per 1000 bp
Lifetimes	Two populations with lifetimes of ~1 and ~6 s	>20 s
Occupancy of pause space (%)	95	5
Phases at high spatial resolution	No phases (sharp transitions into and out of the pause)	Backtracking, pause, and recovery
Load dependence	Independent	Both frequency and duration are strongly force dependent
Effect of inosine triphosphate (ITP)[a]	No effect	Increase in both frequency and duration (phase signature unchanged)
Effect of GreA and GreB	No effect	Reduce both frequency and duration

[a] ITP is a guanine analog forming a weaker Watson-Crick pair, thus decreasing the stability of both the DNA/RNA hybrid and the secondary structures in nascent RNA. Its effects are similar to those of mismatched bases, and thus its incorporation into the RNA transcript can be used to simulate errors of the elongation process in vivo. Since ITP influences both the frequency and duration of the long pauses, and since both of these parameters are affected by GreA/B, it is suggested that the long pauses could serve the function of the long-sought "proofreading" mechanism for RNA polymerases.

masked by noise in records of individual RNAP molecules. To that end, the individual records were aligned by their rising edges, both at the beginning of the pause and immediately before the resumption of elongation. Three successive phases of the long pause were discerned: backtracking at the beginning, pausing per se, and slow recovery (the average velocity of forward movement is ~0.3 bp s^{-1} versus ~13 bp s^{-1} during normal elongation). The duration and frequency of the backtracking pauses were strongly dependent on application of either opposing or assisting force (see the legend of Figure 5 for definitions of these forces). An interesting approach toward understanding the molecular nature and the physiological significance of the backtracked pauses and the resumption of elongation was to perform the experiment in the presence of the ribonucleotide analog inosine triphosphate (see Table 2 for further explanation) and the bacterial proteins GreA and/or GreB, known to stimulate the cleavage of nascent RNA. Indeed, while ITP increased both the frequency and duration of the pauses, GreA and GreB decreased both parameters. The analysis of the data, taken together with existing biochemical data (e.g., Toulokhonov et al., 2001; Erie, 2002) led to the model presented in Figure 6.

Not yet characterized by the application of single-molecule methods are some other interesting types of pauses and regulatory sites. These include sequence-specific pauses (such as those observed at the Ops site), as well as pauses that are induced by changes in RNA secondary structure (e.g., His or Trp pauses) (Artsimovitch and Landick, 2000; Toulokhonov et al., 2001). In addition, the effects of a number of regulatory proteins such as NusA and NusB on pausing need to be studied

by these methods. It should be noted that single-subunit polymerases (T7) also recognize sequence-specific pause/termination sites that respond to regulatory proteins (T7 lysozyme) (Lyakhov et al., 1998; Zhang and Studier, 2004); studying these may help to understand pausing from a broader biological perspective.

To our knowledge, there is only one paper addressing transcription termination by single-molecule techniques (Yin et al., 1999). Using the TPM method and DNA templates containing the terminator sequence from the *E. coli his* gene, the authors observed that the polymerase remains at this terminator sequence for ~1 min before releasing the DNA. The formation of the paused intermediate at this site is both necessary and sufficient to terminate transcription; moreover, the release of the RNA chain and of the DNA template occurs nearly simultaneously. Termination is a nonequilibrium process that can only be fully understood by defining its individual steps and the alternative read-through pathways and by measuring their rates. Thus, caution should be exercised in analyzing biochemical processes by simply determining the energetics of the relevant interactions, without taking into account kinetic factors.

Concluding Remarks

We hope we have been able to convince the reader of the power of applying single-molecule approaches to the very complex process of transcription. These approaches, taken in combination with biochemical results and recent high-resolution structural data, allow for unprecedented insight into the intricacies and idiosyncrasies of RNA polymerases. Still, this is only the beginning. We expect a burst of single-molecule projects aimed at further understanding of transcription and its regulation. The results of such studies will provide a much-needed understanding of the normal functioning of elongation and its alterations in the diseased state.

Acknowledgments

Special thanks go to the anonymous reviewers whose thoughtful comments and suggestions have helped us to improve this manuscript. We thank Drs. Ken van Holde and Miroslav Tomschik for critical reading of the manuscript. The authors are supported by National Science Foundation grant MCB0504239 (J.Z.), National Cancer Institute K22 (S.H.L.), The Pittsburgh Foundation (S.H.L. and J.Z.), The Rett Syndrome Research Foundation (S.H.L. and J.Z.), and National Institutes of Health grants GM038147 (W.T.M.) and GM54098 (S.B.).

References

Abbondanzieri, E.A., Greenleaf, W.J., Shaevitz, J.W., Landick, R., and Block, S.M. (2005). Direct observation of base-pair stepping by RNA polymerase. Nature *438*, 460–465.

Adelman, K., La Porta, A., Santangelo, T.J., Lis, J.T., Roberts, J.W., and Wang, M.D. (2002). Single molecule analysis of RNA polymerase elongation reveals uniform kinetic behavior. Proc. Natl. Acad. Sci. USA *99*, 13538–13543.

Adelman, K., Yuzenkova, J., La Porta, A., Zenkin, N., Lee, J., Lis, J.T., Borukhov, S., Wang, M.D., and Severinov, K. (2004). Molecular mechanism of transcription inhibition by peptide antibiotic Microcin J25. Mol. Cell *14*, 753–762.

Armache, K.J., Kettenberger, H., and Cramer, P. (2005). The dynamic machinery of mRNA elongation. Curr. Opin. Struct. Biol. *15*, 197–203.

Arndt, K.M., and Kane, C.M. (2003). Running with RNA polymerase: eukaryotic transcript elongation. Trends Genet. *19*, 543–550.

Artsimovitch, I., and Landick, R. (2000). Pausing by bacterial RNA polymerase is mediated by mechanistically distinct classes of signals. Proc. Natl. Acad. Sci. USA *97*, 7090–7095.

Ashkin, A. (1997). Optical trapping and manipulation of neutral particles using lasers. Proc. Natl. Acad. Sci. USA *94*, 4853–4860.

Bai, L., Shundrovsky, A., and Wang, M.D. (2004). Sequence-dependent kinetic model for transcription elongation by RNA polymerase. J. Mol. Biol. *344*, 335–349.

Bar-Nahum, G., Epshtein, V., Ruckenstein, A.E., Rafikov, R., Mustaev, A., and Nudler, E. (2005). A ratchet mechanism of transcription elongation and its control. Cell *120*, 183–193.

Borukhov, S., and Nudler, E. (2003). RNA polymerase holoenzyme: structure, function and biological implications. Curr. Opin. Microbiol. *6*, 93–100.

Borukhov, S., Lee, J., and Laptenko, O. (2005). Bacterial transcription elongation factors: new insights into molecular mechanism of action. Mol. Microbiol. *55*, 1315–1324.

Bustamante, C., Macosko, J.C., and Wuite, G.J. (2000). Grabbing the cat by the tail: manipulating molecules one by one. Nat. Rev. Mol. Cell Biol. *1*, 130–136.

Bustamante, C., Chemla, Y.R., Forde, N.R., and Izhaky, D. (2004). Mechanical processes in biochemistry. Annu. Rev. Biochem. *73*, 705–748.

Coulombe, B., and Burton, Z.F. (1999). DNA bending and wrapping around RNA polymerase: a "revolutionary" model describing transcriptional mechanisms. Microbiol. Mol. Biol. Rev. *63*, 457–478.

Cramer, P., Bushnell, D.A., and Kornberg, R.D. (2001). Structural basis of transcription: RNA polymerase II at 2.8 Å resolution. Science *292*, 1863–1876.

Davenport, R.J., Wuite, G.J., Landick, R., and Bustamante, C. (2000). Single-molecule study of transcriptional pausing and arrest by *E. coli* RNA polymerase. Science *287*, 2497–2500.

Erie, D.A. (2002). The many conformational states of RNA polymerase elongation complexes and their roles in the regulation of transcription. Biochim. Biophys. Acta *1577*, 224–239.

Forde, N.R., Izhaky, D., Woodcock, G.R., Wuite, G.J., and Bustamante, C. (2002). Using mechanical force to probe the mechanism of pausing and arrest during continuous elongation by *Escherichia coli* RNA polymerase. Proc. Natl. Acad. Sci. USA *99*, 11682–11687.

Gnatt, A. (2002). Elongation by RNA polymerase II: structure-function relationship. Biochim. Biophys. Acta *1577*, 175–190.

Gnatt, A.L., Cramer, P., Fu, J., Bushnell, D.A., and Kornberg, R.D. (2001). Structural basis of transcription: an RNA polymerase II elongation complex at 3.3 Å resolution. Science *292*, 1876–1882.

Greive, S.J., and von Hippel, P.H. (2005). Thinking quantitatively about transcriptional regulation. Nat. Rev. Mol. Cell Biol. *6*, 221–232.

Guajardo, R., and Sousa, R. (1997). A model for the mechanism of polymerase translocation. J. Mol. Biol. *265*, 8–19.

Gueroui, Z., Place, C., Freyssingeas, E., and Berge, B. (2002). Observation by fluorescence microscopy of transcription on single combed DNA. Proc. Natl. Acad. Sci. USA *99*, 6005–6010.

Guthold, M., Zhu, X., Rivetti, C., Yang, G., Thomson, N.H., Kasas, S., Hansma, H.G., Smith, B., Hansma, P.K., and Bustamante, C. (1999). Direct observation of one-dimensional diffusion and transcription by *Escherichia coli* RNA polymerase. Biophys. J. *77*, 2284–2294.

Harada, Y., Funatsu, T., Murakami, K., Nonoyama, Y., Ishihama, A., and Yanagida, T. (1999). Single-molecule imaging of RNA polymerase-DNA interactions in real time. Biophys. J. *76*, 709–715.

Harada, Y., Ohara, O., Takatsuki, A., Itoh, H., Shimamoto, N., and Kinosita, K., Jr. (2001). Direct observation of DNA rotation during transcription by *Escherichia coli* RNA polymerase. Nature *409*, 113–115.

Holmes, S.F., and Erie, D.A. (2003). Downstream DNA sequence effects on transcription elongation. Allosteric binding of nucleoside triphosphates facilitates translocation via a ratchet motion. J. Biol. Chem. *278*, 35597–35608.

Jülicher, F., and Bruinsma, R. (1998). Motion of RNA polymerase along DNA: a stochastic model. Biophys. J. *74*, 1169–1185.

Kabata, H., Kurosawa, O., Arai, I., Washizu, M., Margarson, S.A., Glass, R.E., and Shimamoto, N. (1993). Visualization of single molecules of RNA polymerase sliding along DNA. Science *262*, 1561–1563.

Kapanidis, A., Margeat, E., Laurence, T., Doose, S., Ho, S., Mukhopadhyay, J., Kortkhonjia, E., Mekler, V., Ebright, R., and Weiss, S. (2005). Retention of transcription initiation factor s70 in transcription elongation: single-molecule analysis. Mol. Cell *20*, 347–356.

Kasas, S., Thomson, N.H., Smith, B.L., Hansma, H.G., Zhu, X., Guthold, M., Bustamante, C., Kool, E.T., Kashlev, M., and Hansma, P.K. (1997). *Escherichia coli* RNA polymerase activity observed using atomic force microscopy. Biochemistry *36*, 461–468.

Komissarova, N., and Kashlev, M. (1997a). RNA polymerase switches between inactivated and activated states by translocating back and forth along the DNA and the RNA. J. Biol. Chem. *272*, 15329–15338.

Komissarova, N., and Kashlev, M. (1997b). Transcriptional arrest: *Escherichia coli* RNA polymerase translocates backward, leaving the 3′ end of the RNA intact and extruded. Proc. Natl. Acad. Sci. USA *94*, 1755–1760.

Landick, R. (1997). RNA polymerase slides home: pause and termination site recognition. Cell *88*, 741–744.

Landick, R. (2004). Active-site dynamics in RNA polymerases. Cell *116*, 351–353.

Leuba, S.H., and Zlatanova, J., eds. (2001). Biology at the single-molecule level (Amsterdam: Pergamon).

Lyakhov, D.L., He, B., Zhang, X., Studier, F.W., Dunn, J.J., and McAllister, W.T. (1998). Pausing and termination by bacteriophage T7 RNA polymerase. J. Mol. Biol. *280*, 201–213.

Marr, M.T., and Roberts, J.W. (2000). Function of transcription cleavage factors GreA and GreB at a regulatory pause site. Mol. Cell *6*, 1275–1285.

Mooney, R.A., Darst, S.A., and Landick, R. (2005). Sigma and RNA polymerase: an on-again, off-again relationship? Mol. Cell *20*, 335–345.

Mukhopadhyay, J., Sineva, E., Knight, J., Levy, R.M., and Ebright, R.H. (2004). Antibacterial peptide microcin J25 inhibits transcription by binding within and obstructing the RNA polymerase secondary channel. Mol. Cell *14*, 739–751.

Murakami, K.S., Masuda, S., and Darst, S.A. (2002). Structural basis of transcription initiation: RNA polymerase holoenzyme at 4 Å resolution. Science *296*, 1280–1284.

Neuman, K.C., and Block, S.M. (2004). Optical trapping. Rev. Sci. Instr. *75*, 2787–2809.

Neuman, K.C., Abbondanzieri, E.A., Landick, R., Gelles, J., and Block, S.M. (2003). Ubiquitous transcriptional pausing is independent of RNA polymerase backtracking. Cell *115*, 437–447.

Nickels, B.E., Garrity, S.J., Mekler, V., Minakhin, L., Severinov, K., Ebright, R.H., and Hochschild, A. (2005). The interaction between sigma70 and the beta-flap of *Escherichia coli* RNA polymerase inhibits extension of nascent RNA during early elongation. Proc. Natl. Acad. Sci. USA *102*, 4488–4493.

Nudler, E. (1999). Transcription elongation: structural basis and mechanisms. J. Mol. Biol. *288*, 1–12.

Nudler, E., Mustaev, A., Lukhtanov, E., and Goldfarb, A. (1997). The RNA-DNA hybrid maintains the register of transcription by preventing backtracking of RNA polymerase. Cell *89*, 33–41.

Pomerantz, R.T., Ramjit, R., Gueroui, Z., Place, C., Anikin, M., Leuba, S., Zlatanova, J., and McAllister, W.T. (2005). A tightly regulated molecular motor based upon T7 RNA polymerase. Nano Lett. *5*, 1698–1703.

Reeder, T.C., and Hawley, D.K. (1996). Promoter proximal sequences modulate RNA polymerase II elongation by a novel mechanism. Cell *87*, 767–777.

Revyakin, A., Ebright, R.H., and Strick, T.R. (2004). Promoter unwinding and promoter clearance by RNA polymerase: detection by single-molecule DNA nanomanipulation. Proc. Natl. Acad. Sci. USA *101*, 4776–4780.

Ring, B.Z., Yarnell, W.S., and Roberts, J.W. (1996). Function of *E. coli* RNA polymerase sigma factor sigma 70 in promoter-proximal pausing. Cell *86*, 485–493.

Rippe, K., Guthold, M., von Hippel, P.H., and Bustamante, C. (1997). Transcriptional activation via DNA-looping: visualization of intermediates in the activation pathway of *E. coli* RNA polymerase·σ^{54} holoenzyme by scanning force microscopy. J. Mol. Biol. *270*, 125–138.

Rivetti, C., Guthold, M., and Bustamante, C. (1999). Wrapping of DNA around the *E. coli* RNA polymerase open promoter complex. EMBO J. *18*, 4464–4475.

Rivetti, C., Codeluppi, S., Dieci, G., and Bustamante, C. (2003). Visualizing RNA extrusion and DNA wrapping in transcription elongation complexes of bacterial and eukaryotic RNA polymerases. J. Mol. Biol. *326*, 1413–1426.

Sakata-Sogawa, K., and Shimamoto, N. (2004). RNA polymerase can track a DNA groove during promoter search. Proc. Natl. Acad. Sci. USA *101*, 14731–14735.

Schafer, D.A., Gelles, J., Sheetz, M.P., and Landick, R. (1991). Transcription by single molecules of RNA polymerase observed by light microscopy. Nature *352*, 444–448.

Schulz, A., Mucke, N., Langowski, J., and Rippe, K. (1998). Scanning force microscopy of *Escherichia coli* RNA polymerase·σ^{54} holoenzyme complexes with DNA in buffer and in air. J. Mol. Biol. *283*, 821–836.

Science (1999). Frontiers in chemistry: single molecules. March issue. Science *283*, 1593–1804.

Shaevitz, J.W., Abbondanzieri, E.A., Landick, R., and Block, S.M. (2003). Backtracking by single RNA polymerase molecules observed at near-base-pair resolution. Nature *426*, 684–687.

Shilatifard, A., Conaway, R.C., and Conaway, J.W. (2003). The RNA polymerase II elongation complex. Annu. Rev. Biochem. *72*, 693–715.

Skinner, G.M., Baumann, C.G., Quinn, D.M., Molloy, J.E., and Hoggett, J.G. (2004). Promoter binding, initiation, and elongation by bacteriophage T7 RNA polymerase. A single-molecule view of the transcription cycle. J. Biol. Chem. *279*, 3239–3244.

Tahirov, T.H., Temiakov, D., Anikin, M., Patlan, V., McAllister, W.T., Vassylyev, D.G., and Yokoyama, S. (2002). Structure of a T7 RNA polymerase elongation complex at 2.9 Å resolution. Nature *420*, 43–50.

Temiakov, D., Patlan, V., Anikin, M., McAllister, W.T., Yokoyama, S., and Vassylyev, D.G. (2004). Structural basis for substrate selection by T7 RNA polymerase. Cell *116*, 381–391.

ten Heggeler-Bordier, B., Wahli, W., Adrian, M., Stasiak, A., and Dubochet, J. (1992). The apical localization of transcribing RNA polymerases on supercoiled DNA prevents their rotation around the template. EMBO J. *11*, 667–672.

Thomen, P., Lopez, P.J., and Heslot, F. (2005). Unravelling the mechanism of RNA-polymerase forward motion by using mechanical force. Phys. Rev. Lett. *94*, 128102.

Tolic-Nørrelykke, S.F., Engh, A.M., Landick, R., and Gelles, J. (2004). Diversity in the rates of transcript elongation by single RNA polymerase molecules. J. Biol. Chem. *279*, 3292–3299.

Toulokhonov, I., Artsimovitch, I., and Landick, R. (2001). Allosteric control of RNA polymerase by a site that contacts nascent RNA hairpins. Science *292*, 730–733.

Tuske, S., Sarafianos, S.G., Wang, X., Hudson, B., Sineva, E., Mukhopadhyay, J., Birktoft, J.J., Leroy, O., Ismail, S., Clark, A.D., Jr., et al. (2005). Inhibition of bacterial RNA polymerase by streptolydigin: stabilization of a straight-bridge-helix active-center conformation. Cell *122*, 541–552.

Uptain, S.M., Kane, C.M., and Chamberlin, M.J. (1997). Basic mechanisms of transcript elongation and its regulation. Annu. Rev. Biochem. *66*, 117–172.

van Holde, K., ed. (1999). Minireview series on single-molecules. J. Biol. Chem. *274*, 14515.

Vassylyev, D.G., Sekine, S., Laptenko, O., Lee, J., Vassylyeva, M.N., Borukhov, S., and Yokoyama, S. (2002). Crystal structure of a bacterial RNA polymerase holoenzyme at 2.6 Å resolution. Nature *417*, 712–719.

von Hippel, P.H., and Pasman, Z. (2002). Reaction pathways in transcript elongation. Biophys. Chem. *101–102*, 401–423.

Wang, H.Y., Elston, T., Mogilner, A., and Oster, G. (1998a). Force generation in RNA polymerase. Biophys. J. *74*, 1186–1202.

Wang, M.D., Schnitzer, M.J., Yin, H., Landick, R., Gelles, J., and Block, S.M. (1998b). Force and velocity measured for single molecules of RNA polymerase. Science *282*, 902–907.

Yin, Y.W., and Steitz, T.A. (2002). Structural basis for the transition from initiation to elongation transcription in T7 RNA polymerase. Science *298*, 1387–1395.

Yin, Y.W., and Steitz, T.A. (2004). The structural mechanism of translocation and helicase activity in t7 RNA polymerase. Cell *116*, 393–404.

Yin, H., Landick, R., and Gelles, J. (1994). Tethered particle motion method for studying transcript elongation by a single RNA polymerase molecule. Biophys. J. *67*, 2468–2478.

Yin, H., Wang, M.D., Svoboda, K., Landick, R., Block, S.M., and Gelles, J. (1995). Transcription against an applied force. Science *270*, 1653–1657.

Yin, H., Artsimovitch, I., Landick, R., and Gelles, J. (1999). Nonequilibrium mechanism of transcription termination from observations of single RNA polymerase molecules. Proc. Natl. Acad. Sci. USA *96*, 13124–13129.

Zhang, X., and Studier, F.W. (2004). Multiple roles of T7 RNA polymerase and T7 lysozyme during bacteriophage T7 infection. J. Mol. Biol. *340*, 707–730.

Zhang, G., Campbell, E.A., Minakhin, L., Richter, C., Severinov, K., and Darst, S.A. (1999). Crystal structure of *Thermus aquaticus* core RNA polymerase at 3.3 Å resolution. Cell *98*, 811–824.

Zlatanova, J., and Leuba, S.H. (2003). Chromatin fibers, one-at-a-time. J. Mol. Biol. *331*, 1–19.

Zlatanova, J., Lindsay, S.M., and Leuba, S.H. (2001). Single molecule force spectroscopy in biology using the Atomic Force Microscopy. Prog. Biophys. Mol. Biol. *74*, 37–61.